

## Power Distribution for Cryogenic Instruments at 6-40K The James Webb Space Telescope Case

Peter Rumler<sup>(1)</sup>, Ray Lundquist<sup>(2)</sup>, Jose Lorenzo Alvarez<sup>(1)</sup>, Jeff Sincell<sup>(2)</sup>, Jim Tuttle<sup>(2)</sup>

<sup>(1)</sup>ESA-ESTEC, 2200AG Noordwijk, Netherlands, peter.rumler@esa.int

<sup>(2)</sup>NASA-GSFC, Greenbelt, MD-20771 USA, ray.a.lundquist@nasa.gov

### ABSTRACT

The Integrated Science Instrument Module (ISIM) of the James Webb Space Telescope (JWST) operates its instruments passively cooled at around 40 Kelvin (K), with a warm Instrument Electronic Compartment (IEC) at 300K attached to it. From the warm electronics all secondary signal and power harnesses have to bridge this 300-40K temperature difference and minimize the power dissipation and parasitic heat leak into the cold region.

After an introduction of the ISIM with its instruments, the IEC with the electronics, and the harness architecture with a special radiator, this paper elaborates on the cryogenic wire selection and tests performed to establish current de-rating rules for different wire types. Finally failure modes are analyzed for critical instrument interfaces that could inject excessive currents and heat into the harness and cold side, and several solutions for the removal of such failures are presented.

### 1. INTRODUCTION

The James Webb Space Telescope (JWST) is an Infrared Space Observatory that will follow-up Hubble in 2016, designed by NASA with contributions from ESA and the Canadian Space Agency (CSA). ESA provides the Ariane-5 Launch vehicle for JWST and supplies the Near Infrared Spectrograph (NIRSpec) and the science part of the Mid Infrared Instrument (MIRI). CSA provides an instrument with a Fine Guidance Sensor (FGS) and tuneable Filter. JWST features a sunshield approximately the size of a tennis court that passively cools the Integrated Science Instrument Module (ISIM) with the infrared instruments.

Figure 1 shows JWST in stowed (launch) configuration without the sunshield and the three thermal regions where instrument components are located.

### 2. ISIM OVERVIEW

The ISIM is the Payload Element of the JWST, containing the Near-Infrared Camera (NIRCam), NIRSpec, MIRI, and FGS. The optical assemblies (OA) of the instruments contain the optics, the respective Focal Plane Assemblies (FPA) with infrared detectors and mechanisms, and they are mounted to the

ISIM structure located in Region 1 of the JWST Observatory. Each instrument's OA is connected through a heat strap to a dedicated radiator that provides passive cooling to temperatures below 40K. In addition, the NIRSpec FPA and the SIDECAR ASIC (System for Image Digitization, Enhancement, Control and Retrieval) connect to a dedicated radiator separate from the NIRSpec OA radiator. The ISIM Structure is a frame made of square graphite fiber reinforced plastic (GFRP) tubes attached together with gussets and clips, and with metal fittings for the Optical Telescope Element (OTE) and Science Instrument interfaces. The resistivity of the GFRP tube material has been measured to be in the order of  $1\Omega/m$ , and the resistance of the joints between GFRP tubes has been measured to be approximately  $10-20\Omega$  per joint. The resulting overall ISIM structure resistance of  $10-100\Omega$  from the OAs to the IEC ground cannot be considered as a low impedance ground plane in Region 1.

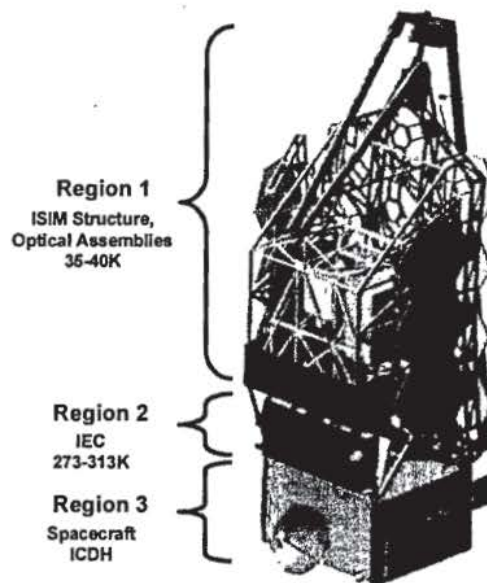


Figure 1. ISIM Component Regions on the JWST Observatory

#### 2.1 Instruments Electronics Compartment (IEC)

The control electronics for each instrument are contained in the IEC, where the temperature will be

maintained between 273K and 313K. The large temperature gradient between Region 1 and Region 2 requires the use of thermally resistive materials to prevent heat transfer.

As a result, all harnesses between Regions 1 and 2 are cryogenic harnesses that will have relatively high wire and shield electrical resistance. Still, they provide a better ground connection between Regions 1 and 2 than the structure. The ground impedance is in the order of 1-10 $\Omega$  when using all shield wires (mostly stainless steel shields) in parallel for one instrument. Figure 2 shows the layout of ISIM and IEC with the interconnecting harnesses.

In addition to the instrument control electronics, the IEC contains the ISIM Remote Services Unit (IRSU), which provides SpaceWire interfaces to the instrument Focal Plane Electronics (FPE) for science data transmission, as well as thermal control for ISIM Region 1. The command and data handling functions for the instruments are provided by the ISIM Command and Data Handling (ICDH) unit in Region 3 via a MIL-1553 bus. And the Power Control Unit (PCU) in the spacecraft supplies all electronic boxes with a 30V unregulated power bus, with a minimum of 22V and a maximum of 35V.

The mass estimate for the IEC compartment is 102kg and 132kg for all electronic boxes inside.

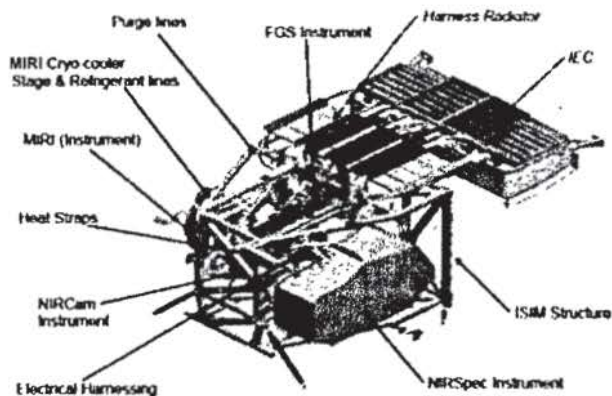


Figure 2. ISIM, IEC and Harness Radiator Layout

## 2.2 Instruments and ISIM Electronics

### NIRCcam

NIRCcam is a large field of view imager that is passively cooled to 37K. NIRCcam contains 10 Sensor Chip Assemblies (SCAs), each of which is controlled by a SIDE CAR ASIC, developed by Rockwell Scientific for JWST operation at 35-40K. Each of the 2 NIRCcam FPE modules in Region 2 controls the interface to 5 SIDE CAR ASICS in Region 1, and it interfaces to the IRSU over SpaceWire. The NIRCcam Instrument Control Electronics (ICE) box controls the mechanisms in Region 1.

### NIRSPEC

NIRSPEC is a large field of view spectrograph that contains 2 SCAs passively cooled to 38K, each of which is controlled by a SIDE CAR ASIC. The NIRSPEC FPE controls the SIDE CAR ASICS, and it interfaces to the IRSU over SpaceWire. The NIRSPEC ICE box controls the mechanisms in Region 1 with the exception of the Microshutter Array (MSA), which is managed by the NIRSPEC Microshutter Control Electronics (MCE) box.

### FGS Guider and Tuneable Filter

The FGS-Guider is used to facilitate fine pointing of the Observatory by providing the Spacecraft with the precise location of a guide star's image in its field of view at 16Hz. FGS includes three separate chains: Guider-1, Guider-2 and the Tuneable Filter (TF). Each chain consists of one SCA with associated SIDE CAR ASIC, and a dedicated FPE/ICE module in the FGS electronics box in the IEC.

### MIRI

MIRI is a combined imager and spectrometer that uses an additional cryo-cooler to actively cool its structure to approximately 7K and its SCAs to 4-6K. The MIRI SCAs make use of a different technology suitable for the medium infrared range, and they are not compatible with the SIDE CAR ASICs. Here the FPE directly controls the SCAs via an analog interface, and provides science data to the IRSU over SpaceWire. The MIRI ICE box controls the MIRI mechanisms in Region 1 with the exception of the cooler. The cooler is controlled by the two Cooler Control Electronics (CCEs for Joule Thomson and Pulse Tube coolers) boxes in Region 3.

### IRSU & ICDH

The IRSU includes a Multi-SpaceWire Concentrator (MSC) with 3 parallel SpaceWire links to the ICDH and the ISIM thermal control electronics. It monitors the Region 1 cryogenic temperature sensors and provides power to the contamination control heaters on the instrument OAs. The contamination control heaters maintain the temperatures of critical components above the temperature of the surrounding structure during cool-down. The MSC also distributes a 60MHz clock to the FPEs and synchronization clocks (100/200/500 kHz) to all instrument electronic boxes.

The ICDH contains the ISIM Flight Software and each instrument's Flight Software Application, as well as the SpaceWire interfaces to the IRSU and the ISIM 1553 bus interfaces to the control electronics. On the other side the ICDH interfaces to the Solid State Recorder (SSR) over SpaceWire and to the Spacecraft Command and Telemetry Processor (CTP) over the S/C-ISIM 1553 Bus (see Fig. 3).



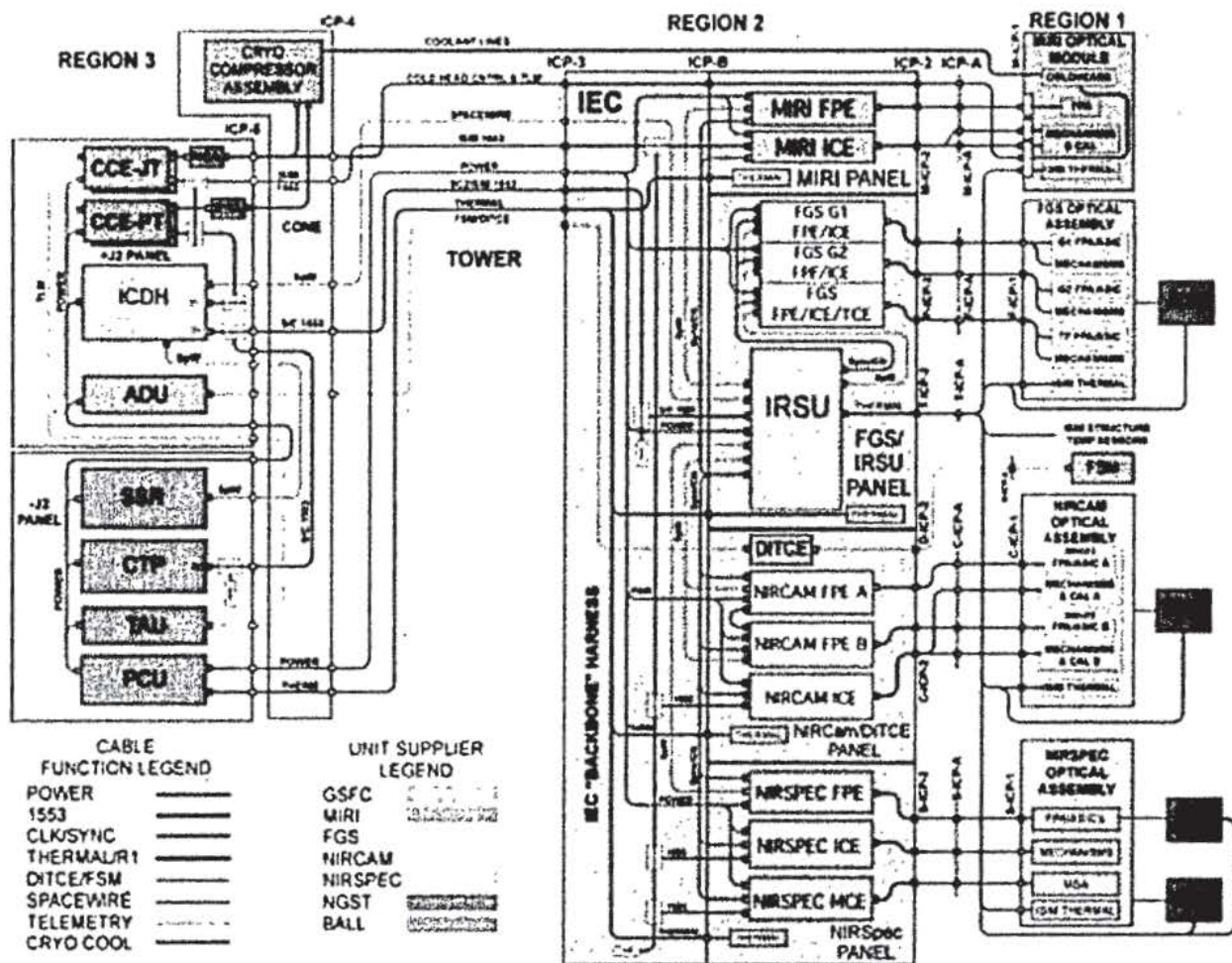


Figure 3. ISIM Electrical Connection Diagram

### 3. HARNESS ARCHITECTURE

The Region 1 harnesses include all the harnesses on the instrument OAs and the ISIM Structure, as well as the harnesses connecting between the ISIM structure and the IEC via the tray radiator. The boundary to Region 2 is at Interface Connector Panels (ICPs) called ICP-2's on the IEC. All harnesses from there up to the interfaces on the instrument OAs (ICP-1's) are cryogenic harnesses that must accommodate the large temperature gradient (300K - 40K). Harnesses inside the IEC and on the instrument OAs are isothermal and can be made of copper. The exception is MIRI where there is a need for cryogenic harnesses from the ISIM mounting interface and ICP-1 at 40K up to the actively cooled OA at 6K. For the ease of integration and testing another series of interface connector panels (ICP-A's) has been introduced between the harness radiator and the ISIM enclosure. With this the ISIM Structure, harness radiator and the IEC can be integrated, tested, and handled separately.

Region 2 harnesses comprise all harnesses inside the IEC. On the Spacecraft side they connect the electronics boxes to the Region 3 interface (power, SpaceWire, 1553-bus and clock/sync) on ICP-3 via the common IEC cavity, which is called the IEC Backbone.

The power harnesses are made of AWG-20 copper wires, with at least two parallel wires for electronics with low power consumption, and up to 10 parallel wires for the IRSU with a peak power consumption of 165W. With a one-way length of 15-16m between the PCU and the electronics in the IEC, this results in a maximum roundtrip voltage drop of no more than 0.75V (at peak power and 22V at the interface). This leads to a total of 67 AWG-20 pairs of power feeds for the 12 electronic boxes with 21 power interfaces. For an average IEC power consumption of 200W (overall peak power is 535W) this seems to be oversized, but the dimensioning had to be done for the individual peak power and voltage drop minimization.



Considering that this significant power cable trunk has to be routed across a deployable tower, the choice for a 28V unregulated power bus no longer seems to be optimal. It has to be noted that the scientific instrument specifications and developments were started much earlier than the spacecraft, and many of these interfaces, such as power, were based on historic designs.

The mass estimate for the thermal and instruments cryogenic harnesses from IEC (ICP-2) to the instrument skin connectors is 10.4kg; and the estimate for the Region 2 power and data distribution harnesses is 28.6kg.

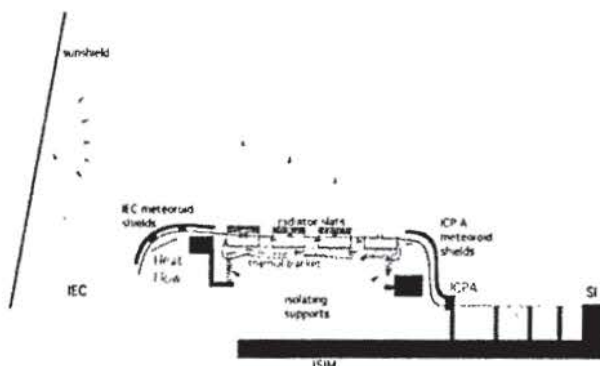


Figure 4. Harness Radiator Thermal Schematic

### 3.1. Harness Radiator

A Harness Radiator (HR) is used to remove the major part of the harness parasitic heat before it can be conducted into the ISIM enclosure and to the science instrument (SI) OAs. For this heat rejection there is a need for a view to deep space, and segments of about 1m of all harnesses are passing through this radiator that is located on the exterior of ISIM, in between the IEC and the ISIM enclosure (see Fig. 2 and Fig. 4). With the harnesses exposed to space in such a way, there is a need to protect them from meteoroid damage and the plasma environment (space charging).

The meteorite shield consists of two 1mm thick aluminium layers, separated by 1cm, with a radiating surface on the outer layer. This provides meteorite protection with a 0.9994 probability of success. And against space charging the outer layer of all harnesses has been made with 5mil Kapton®-XC.

The radiator itself is made of four "slats" that radiate into deep space and are heat sunk to harnesses via clamps. They also absorb radiative back-loading from the sunshield. This design maximizes the thermal isolation of the slats from each other and the backplane support frame of the telescope (BSF). In total the radiator is designed to limit the heat conduction into the ISIM enclosure and the instruments to less than 90mW (150mW max) and the heat conduction into the BSF to 63mW. With this the radiator manages to

reduce the temperature of the harnesses from around 300K at the IEC (ICP-2) to about 60K when entering the ISIM enclosure. The total heat dissipation of the ISIM enclosure, radiated to deep space via the ISIM instrument radiators, is estimated to 490mW. The mass estimate for the harness radiator is 37kg.

### 4. CRYOGENIC WIRE SELECTION & TRADE-OFF

Copper harnesses are not suitable to electrically connect the control electronics in Region 2 (~300K) to the front-end electronics, mechanisms and sensors on the OAs in Region 1 (~35K). Copper has a very high thermal conductivity, which would allow a tremendous amount of heat to flow from Region 2 to Region 1, thus increasing the temperature of the OAs and reduce performance of the near infrared and mid-infrared sensors. For this reason, the harnesses between Region 2 and Region 1 were made of special thin cryogenic wires that minimize heat transfer. Following a trade-off of cryogenic wires physical properties, the type and size of the wire material were carefully chosen by each instrument to meet the electrical performance requirements, as well as the thermal requirements.

In general Stainless Steel wires (SST) were selected for shields and very low current signal lines like thermistors, where an increased voltage drop is of less importance due to the use of bridge acquisition circuits. Temperature sensor mostly use American Wire Gauge (AWG)-38 SST wires with a resistance of about 85Ω/m at ambient that decreases by about 20% at 50K.

Manganin (MN) wires are similar to SST wires, with a little lower resistivity but higher thermal conductivity, and their main feature is a nearly unchanged resistivity over temperature. For JWST they are only used in some detector harnesses for this reason.

For wires that need to carry more current, like secondary power lines for heaters, motors and calibration lamps, Phosphor-Bronze (PhBr) wires have been chosen. Their current capability is much better than for Manganin and SST wires with the same diameter, and a PhBr AWG-28 motor supply wire has a resistance of about 1.4Ω/m at ambient that decreases by about 18% at 50K. This change in harness resistance is quite low compared to the copper motor windings, where the nominal resistance drops by about a factor of 100 from 300K to 35K. One of those cases is the MIRI-Filter Wheel synchro-motor, where the motor coil resistance changes from 370±20Ω at ambient to 3.3±0.2Ω at 4K minimum operational temperature. In order to cope with this wide range of load resistance an additional DC/DC converter is needed in the MIRI ICE, generating a dedicated higher motor driver supply voltage for ambient operations.

## 5. WIRE HEATING AND DERATING TEST

As there are no formal de-rating rules for cryogenic wires, the JWST project started with the maximum de-rated currents for copper wires in bundles as specified in NASA GSFC Preferred Parts list PPL-21 (equivalent to MIL-STD-975 M). An empirical model was generated for small wire gauges below AWG-30, since de-rating rules for copper typically stop at AWG-30 or AWG-32. The allowable currents for SST, PhBr and MN were then derived from the copper de-rated bundle values by scaling them proportional to the specific resistances ( $\Omega/\text{cm}$ ), and rounding them to the closest available wire gauge. In order to verify this de-rating rules for the specific JWST case and layout, a test with

representative PhBr, SST and MN wires was performed in a configuration with bundles and Multi Layer Insulation (MLI) blanketing.

In the particular JWST design the harnesses are first un-blanketed across the harness radiator. Upon entering the ISIM enclosure the wire bundles can be wrapped with MLI blankets in order to avoid becoming sources of infrared stray-light ( $>60\text{K}$ ). This layout, optimized for in-orbit cryogenic operation however, poses a problem for ambient testing, where heat rejection is hampered by the blanketing.

The performed ohmic heating tests simulated this configuration with three different test wire bundle configurations: un-wrapped, wrapped with Teflon® tape, and wrapped with MLI (blanketed).



Figure 5. The unwrapped test harness suspended on the test apparatus

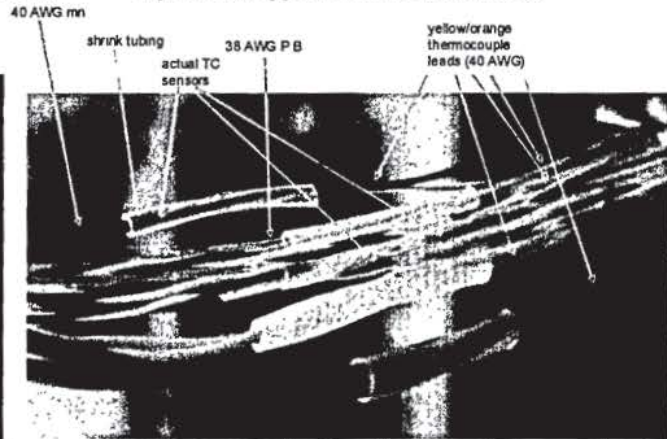


Figure 6. A close-up view of the test harness showing the thermocouple sensors attached to the twisted pairs using heat-shrink tubing

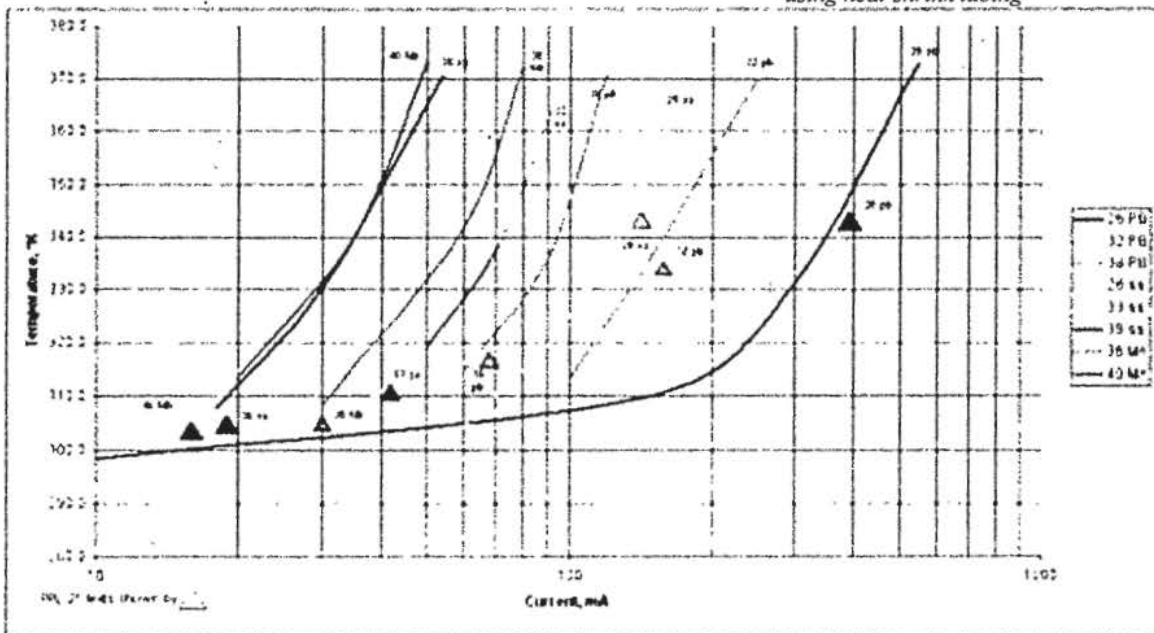


Figure 7. Applied Current versus Wire Temperatures for MLI blanketed Case, compared to PPL-21 limits



**Table 1**  
Max current limits, wrapped, blanketed case  
Pd = 0.00133 W/cm T max = 340°K

AWG	Cu	PB	S304	Mang
26	0.930	0.388	0.153	0.188
28	0.737	0.308	0.122	0.149
30	0.585	0.244	0.096	0.118
32	0.468	0.195	0.077	0.095
34	0.369	0.154	0.061	0.074
36	0.292	0.122	0.048	0.059
38	0.234	0.098	0.039	0.047
40	0.181	0.076	0.030	0.037

The 3 meter long wire bundles were constructed to approximate the design of a typical JWST ICE harness. It contained one twisted pair of each of the following wire types: AWG-26 PhBr(PB), AWG-32 PhBr, AWG-38 PhBr, AWG-26 SST(S304), AWG-33 SST, AWG-38 SST, AWG-36 MN(Mang), and AWG-40 MN. These wires came from various sources and included several different types of Teflon insulation, including: FEP (fluorinated ethylene propylene), PFA (perfluoroalkoxy), TFE (tetrafluoroethylene), and RNF-100 heat-shrink tubing. Each twisted pair was fitted with a thermocouple sensor at the center point (see Fig. 5), shorted on one end, and fitted with copper jumpers on the other end. In this configuration the harness was suspended by tiny strings inside a vacuum chamber (see Fig. 6) and connected via the copper jumpers to the external power supply. Four levels of steady state current were applied in sequence to one twisted pair at a time, and temperatures of all pairs were measured after stabilization. The maximum applied currents were such that the highest temperature measured was close to 100°C (372K).

The results for the test case with Teflon wrapping show somewhat lower temperatures (or slightly higher current) than the unwrapped case, since the Teflon wrapping spreads the heat more evenly between powered and un-powered wires. And for the MLI blanketed test case all wires powered and un-powered showed very similar temperatures within a couple of Kelvin, indicating a nearly isothermal environment inside the MLI and much longer settling times. The bundle diameters were approximately 0.5cm for the Teflon wrapped configuration and about 1cm for the MLI blanketed case. On average the difference in maximum current (at around 100°C) between the Teflon wrapped and MLI blanketed cases was a factor of two. Fig. 7 shows the current versus temperature test results for the MLI blanketed case, and includes the PPL-21 limits (triangles). It also reveals that the PPL-21 limits are more conservative for smaller gauges (lower temperatures), and this indicates that smaller gauges can tolerate a proportionally higher current because the surface area to wire diameter is higher, and

**Table 2**  
Max current limits, wrapped, unblanketed case  
Pd = 0.00525 W/cm T max = 340°K

AWG	Cu	PB	S304	Mang
26	1.848	0.771	0.305	0.373
28	1.465	0.611	0.242	0.296
30	1.162	0.485	0.192	0.235
32	0.930	0.388	0.153	0.188
34	0.732	0.306	0.121	0.148
36	0.581	0.242	0.096	0.117
38	0.465	0.194	0.077	0.094
40	0.360	0.150	0.059	0.073

the generated heat is better conducted to the other bundle wires.

For establishing the new de-rating limits the following assumptions were made:

- The bundle temperature is determined by power density no matter how the power is generated
- The limits for all gauges are adjusted to produce a power-per-unit-length of 1.33 mW/cm (per single wire; 2.66 mW/cm for a pair).
- This value is consistent with a maximum bundle temperature of approximately 340K in a 1cm diameter cable based upon the wrapped-and-blanketed test results. The 340K value was chosen to allow operation above the "knee" of the temperature-versus-current curve (Fig. 7), but retaining some margin for unexpectedly higher stress levels.
- A similar set of limits is derived for wrapped but unblanketed bundles using 5.25mW/cm for a bundle diameter of 0.5cm.

The resulting wire current limits for AWG-26 through AWG-40 in four materials appear in Tables 1 and 2.

In summary the new limits - compared to PPL-21 limits - allow a bit higher currents for wire gauges smaller than AWG-26 for the blanketed case and approximately twice those amounts of current for the un-blanketed case.

Several cautions are associated with these results. The limits established, based upon the test data and an understanding of the physical condition of the harnesses under study here, are higher than PPL-21 would suggest. These limits apply only to tightly wrapped cables where the individual wires are in close physical contact with each other over the length of the cable. Bundle diameter is also important, and cables significantly smaller than the test cable will reach higher internal temperatures because of the smaller radiative surface area of the bundle.

Finally, it was decided to heat the wires inside the harness to a significantly higher temperature to see if any damage would be seen. A current of 0.175A was applied to the AWG-33 SST pair (nearly twice the



amount of 95mA that resulted in 368K during the blanketed test), and the harness wire midpoint sensors eventually reached a temperature of about 465K. The inner and outer MLI sensors read 381K and 373K, respectively. After the test the wires were inspected, and a powdery substance sticking to the wires and the inside of the Teflon wrap was found. On closer examination, the powder was seen to be small clear crystals. This crystalline substance has been analyzed by GSFC's materials group. Preliminary results indicate that it is a flame retardant associated with the heat shrink tubing used in the test article.

## 6. NIRSpec AND MIRI INSTRUMENT CRYOGENIC HARNESSSES

As examples of cryogenic wire selection the harnesses for the NIRSpec and MIRI instruments are presented, followed by an analysis of the failure cases that could lead to wire overheating and failure propagation.

Table 3 shows a summary of the cryogenic wire types and their use for NIRSpec and MIRI. It also includes the measured harness resistances where available, the motor coil resistances and maximum nominal and failure currents, and compares them to the de-rated currents derived in section 5.

Table 3. NIRSpec and MIRI Cryogenic Wire Resistances and Currents

NIRSpec								Minimum motor coil resistance		Cryo Currents			Ambient Currents			Derated Currents			
load	type	conductor	AWG	n <sup>o</sup>	parallel length [m]	R <sub>meas</sub> [Ω]	R <sub>bridge</sub> [Ω]	R <sub>bridge</sub> decrease [%]	R <sub>motor-coil</sub> [Ω]	R <sub>motor-amb</sub> [Ω]	I <sub>max</sub> [mA]	I <sub>max/ste</sub> [mA]	I <sub>failure</sub> [mA]	I <sub>max</sub> [mA]	I <sub>max/ste</sub> [mA]	I <sub>failure</sub> [mA]	I <sub>derated</sub> [mA]	I <sub>max/ste</sub> [mA]	
FWA/GWA	motor drive	PhBr	28	2	4.35	5.83	5.10	12.4%	0.90	74.0	800	283	0	430	152	0	308	611	
RMA	motor drive	PhBr	28	1	4.37	5.81	5.10	12.2%	1.45	49.4	190	190	1099	121	121	238	308	611	
CAA	lamp supply	PhBr	36	1	4.41	58.8	51.2	13.0%			20	20	37	20	20	37	122	242	
FWA/GWA	sensor(pos)	SST	38	1	4.36	373	308	17.3%			10	10	11.3	10	10	11.3	39	77	
FWA/GWA	sensor(temp)	SST	38	1	4.36	373	308	17.3%			1.0	1.0	1.3	1.0	1.0	1.3	39	77	
MIRI								Minimum motor coil resistance		Cryo Currents			Ambient Currents			Derated Currents			
load	type	conductor	AWG	n <sup>o</sup>	parallel length [m]	R <sub>meas</sub> [Ω]	R <sub>bridge</sub> [Ω]	R <sub>bridge</sub> decrease [%]	R <sub>motor-coil</sub> [Ω]	R <sub>motor-amb</sub> [Ω]	I <sub>max</sub> [mA]	I <sub>max/ste</sub> [mA]	I <sub>failure</sub> [mA]	I <sub>max</sub> [mA]	I <sub>max/ste</sub> [mA]	I <sub>failure</sub> [mA]	I <sub>derated</sub> [mA]	I <sub>max/ste</sub> [mA]	
GSE heater	heater supply	PhBr	30	2	5.28	5.98					230	115	175					244	485
POM heater	heater supply	PhBr	30	1	5.81	13.0					30	30	75					244	485
FW	motor drive	PhBr	30	2	6.82	8.01	7.02	as NIRSpec	3.1	350	300	106	1471	140	49.5	213	244	485	
CCC	motor drive	PhBr	30	1	6.82	16.1	14.1	as NIRSpec	2.9	381	100	100	1278	75	75.0	194	244	485	
CF/CI	lamp supply	PhBr	30	1	6.90	16.0					20	20	50	20	20.0	50	244	485	
FW	sensor(pos)	SST	38	1	6.82	637					1.5	1.5	25	1.5	1.5	25	39	77	
CF/CI	sensor(temp)	SST	38	1	6.90	641					1.0	1.0	0.3	1.0	1.0	0.3	39	77	

### 6.1. Failure Mode Considerations

The failure currents for temperature and position sensors with SST wires are all well within the de-rated currents; and the same is valid for the PhBr wires supplying the Calibration Lamps (CAA, CF/CI).

The critical cases are the secondary power interfaces supplying the motor drive currents. For those interfaces a detailed failure mode analysis was performed, including failures in the motor drivers, as well as harness or load short circuits. In case of failure mode currents exceeding the de-rating of the wires, the failure has to be detected and removed by hardware or software function within a relatively short period of time in order to prevent overheating.

For normal failure propagation considerations it could be argued that no de-rating applies in case of a failure, since the function is already lost, and only failure propagation has to be prevented. But for the specific case of JWST a main concern is to limit the thermal dissipation in all cases, including failures. Therefore we have applied current de-rating limits also for failure cases, and any failure generating currents exceeding those limits has to be isolated and removed. In the following sections both load short circuits and motor driver failures are checked for the motor supplies.

### 6.2. NIRSpec Motor Interface Failure Modes

Load short circuits:

During cryogenic operations the motor coil resistance (<2Ω) is lower than the harness resistance (>10Ω), and therefore a harness short is the most severe case. For all motor drivers the current is controlled dynamically by the FPGA independently of the load seen by the ICE, and the current will not exceed its preset value in case of an external short circuit.

Motor driver failures [1]:

a) H-bridge motor drivers for Filter Wheel (FWA) and Grating Wheel (GWA): If a short circuit occurs in the bridge higher branches MOSFET, the current will flow directly from the motor driver supply voltage to the return via an internal low impedance path. No current will therefore flow through motor leads. This is regardless if this occurs during motor movement (when the 4 MOSFET bridge status is controlled by the FPGA) or during steady state (when the bridge lower branches MOSFETs are permanent on), no failure current is injected towards the motors. In addition, due to the short between drivers supply and return, the DC/DC converter will switch off.

b) Linear motor driver for Refocusing Mechanism (RMA): The output stage is based on bipolar transistors. In case of emitter-collector short circuit of the transistor, the maximum current provided to the motor is only limited by the resistances of the harness, motor coil and current sensing resistors. This failure current can be as high as 1100mA in cryogenic



conditions, where the motor coil resistance is lowest. Since this current exceeds the de-rated value of 308mA (blanketed) for AWG-28 PhBr wires, a software monitoring circuit was introduced to isolate this failure within 12.5 seconds. In ambient conditions the failure current is only 238mA due to the much higher motor coil resistance, and is within the wire de-rating limit. Also for this failure event the software monitoring will remove the failure.

### 6.3. MIRI Motor & Heater Interface Failure Modes Load short circuits:

As for NIRSpec the MIRI motor controllers limit the motor current to the set maximum values in case of a short circuit in the harness or motor windings. Also the heater supplies are current limited: For the Pick-Off-Mirror (POM) there is a current limiter in the driver circuit that limits the current to 75mA, and the Ground Support Equipment (GSE) power supply current limit is set to 350mA (175mA per wire), which is well below the wire de-rating.

#### Motor driver failure:

Due to the relatively low drive currents for the MIRI Filter Wheel (FW) and Contamination Control cover (CCC) mechanisms all motor drivers in the MIRI ICE use linear amplifiers. As for NIRSpec, those drivers have a transistor (MOSFET) failure mode that shorts the supply voltage (80V ambient, 40V cryogenic) to the output. In ambient a much higher motor coil resistance limits the failure currents to 202mA maximum, which is below the de-rated value (244mA) for the used PhBr AWG-30 wires. In cryogenic condition the over-current is limited only by the DC/DC converter limit and a 10Ω shunt resistor at the driver output. The DC/DC converter can supply up to 40W (1A), and in case of a load resistance less than 40Ω a hardwired Hiccup Mode incorporated in the ICE will start to limit the failure current and dissipation to 10%.

Figure 8 shows the operations of the HICCUP Mode, that works as follows: The MIRI ICE DC/DC converters are protected against overload and output short circuit, and can deliver a maximum current of 1A. Up to this limit the converter is operating in voltage-regulated mode, and beyond this limit the DC/DC goes into current limitation mode and the output voltages fall. When the output voltages are falling below ~30% of the nominal value the supply goes in the Hiccup Current Limitation Mode, meaning that the DC/DC converter will alternate current limitation mode during 10mS with 90mS of stopping, and so on. In that way the hiccup mode generates 10% of the average power dissipation of current limitation mode. The drawback is that the power bus will be subject to low frequency, high peak current pulses.

This means that if the total load ( $R_{\text{harness}} + R_{\text{coil}} + R_{\text{harness}} + R_{\text{shunt}}$ ) is smaller than ~40Ω (cryogenic case) the

motor supply DC/DC converter goes into hiccup mode. The failure is detected by ICE internal monitoring of the secondary voltages telemetry, which is acquired every 10ms: Then the 40V or 80V power supplies are alternatively turned off during ~90ms and on during ~10ms. And the motor coil is then fed with 1A during ~10ms every ~100ms (100mA average), until the motor supply DC/DC converter is switched off by external software monitoring.

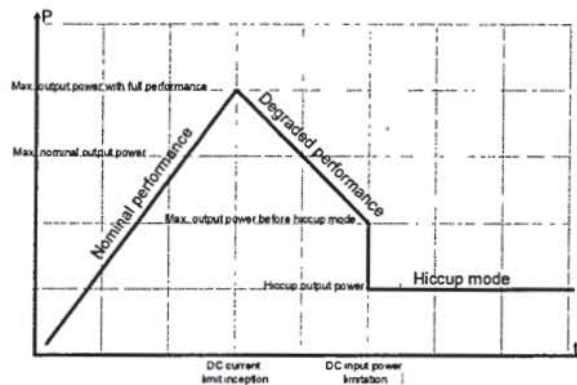


Figure 8. Hiccup Mode diagram

When the total load is bigger than ~40Ω (ambient case) the driver may feed the coil with up to ~1A and generate a continuous over-dissipation. In this case the motor coils are supplied with abnormally high voltages (up to +40V/+80V). This is detected by the motor coil voltage telemetry, and the software will turn off the motor feeding DC/DC converter. But also here the ambient failure case generates over-currents below the de-rating limits as already mentioned above.

## 7. CONCLUSION

The JWST ISIM electrical architecture has been presented with emphasis on the cryogenic power distribution and harnesses. The cryogenic wire selection was discussed together with a dedicated test to derive current de-rating recommendations. And finally critical failure modes in the instrument motor supplies have been analyzed and failure isolation strategies were presented.

## 8. REFERENCES

1. Rumler P., et al, Motor Control Electronics for NIRSpec Cryogenic Mechanisms on JWST, In proceedings of 8<sup>th</sup> European Space Power Conference, Konstanz, Germany, September 2008